

Goldilocks RL: Tuning Task Difficulty to Escape Sparse Rewards for Reasoning

Ilia Mahrooghi^{†1}, Aryo Lotfi², and Emmanuel Abbe^{1,2}

¹*EPFL*

²*Apple*

Abstract

Reinforcement learning has emerged as a powerful paradigm for unlocking reasoning capabilities in language models. However, relying on sparse rewards makes this process highly sample-inefficient, as models must navigate vast search spaces with minimal feedback. While classic curriculum learning aims to mitigate this by ordering data based on complexity, prior works have primarily targeted small datasets and do not directly transfer to the large-scale settings typical of modern LM training. Furthermore, the right ordering for a specific model is often unclear. To address this, we propose Goldilocks, a novel teacher-driven data sampling strategy that aims to predict each question’s difficulty for the student model. The teacher model selects questions of appropriate difficulty for the student model, i.e., questions that are neither too easy nor too hard (Goldilocks principle), while training the student with GRPO. By leveraging the student’s performance on seen samples, the teacher continuously adapts to the student’s evolving abilities. On the OpenMathReasoning dataset, Goldilocks data sampling improves the performance of models trained with standard GRPO under the same compute budget.

1 Introduction

The reasoning capabilities of Transformer-based models have been a focal point of recent research, with Reinforcement Learning (RL) emerging as a powerful paradigm for enhancing these abilities. Recent RL methods incentivize the generation of a detailed Chain of Thought (CoT) [30], enabling models to solve complex problems [38, 7, 10]. Additionally, increasing the computational budget at inference time, known as scaling test-time compute, has been shown to further enhance these reasoning capabilities [26, 19]. While RL has proven effective in unlocking complex reasoning behaviors, the computational efficiency of these methods remains a significant challenge. Recent findings by Khatri et al. [11] underscore that scaling is a fundamental driver of performance. This observation suggests that while models have the potential for continued improvement, realizing this potential through brute-force scaling is resource-intensive, making training efficiency a paramount concern.

Outcome Supervision (OS) [6, 36] further complicates this efficiency landscape. OS rewards the model only if the final answer is correct, creating a sparse reward signal where the model receives no feedback during intermediate reasoning steps. Because of this sparsity, the model must explore a vast number of reasoning paths to stumble upon a correct solution. This need for extensive exploration to find a positive signal makes learning slow and resource-intensive, serving as another critical motivation for improving the efficiency of RL training methods.

Curriculum Learning (CL) [4] addresses these inefficiencies by presenting training examples in a meaningful order rather than a random one. Recent work [22, 21, 25, 5, 35] has explored various strategies for selecting and scheduling data in language model training, but relies on two recurring assumptions. Many approaches are *history-based*, estimating sample difficulty by tracking a model’s past performance on specific instances where it’s feasible only when the dataset is small enough to traverse repeatedly. Others assume the dataset is partitioned into predefined difficulty categories and schedule at the category level. More recent efforts attempt to mitigate the cost of uninformative samples by performing rollouts and skipping the policy update when they prove non-informative [29, 32], but this

[†]Corresponding Author, ilia.mahrooghi@epfl.ch

still incurs the full GPU cost of generation. Gu et al. [9] move beyond history-based heuristics with a bandit-based co-adaptive curriculum, but their method remains targeted at small-scale datasets.

Both assumptions break down at the scale of modern LM training, where corpora are traversed only once and rarely come with difficulty labels. Revisiting examples just to estimate their difficulty wastes GPU resources, history-based methods provide no signal for unseen data, and category-based scheduling is unavailable. Standard CL methods are therefore not just suboptimal in this regime but **inapplicable**, and cannot serve as direct baselines in our setting. We treat **closing this gap as part of our contribution**, proposing a strategy that judges and schedules new data on the fly without prior training passes or auxiliary annotations.

In this work, we propose **Goldilocks**, a novel teacher-driven framework where, in parallel with training the student model, a teacher continuously learns the student’s current capabilities and selects questions of appropriate difficulty — neither too easy nor too hard. The teacher generalizes to new data streams the student has not seen, building a curriculum tailored to the student at each point in training. This design removes both bottlenecks of prior CL methods: the student does not need to see each instance multiple times, and the teacher does not rely on category structure in the data.

The paper is organized as follows. Section 2 analyzes GRPO [24] gradient dynamics under verifiable rewards. Section 3 presents our joint training framework, and Section 4 the Teacher–Student architecture. Sections 5 and 6 report empirical results and ablations. Section 7 discusses related work, and Section 8 concludes.

2 Theoretical Motivation: The Goldilocks Zone

In the context of fine-tuning language models with RL, the objective is to maximize the expected reward on a dataset of verifiable answers. The standard policy gradient loss is defined as

$$\mathcal{L}_{PG} = -\mathbb{E}_{s_t, a_t} \left[\log \pi_{\theta}(a_t | s_t) \hat{A}_t \right],$$

where π_{θ} denotes the policy and \hat{A}_t represents the estimated advantage. In the context of updating language models, the state s_t corresponds to the prompt q combined with the history of generated tokens $o_{<t}$, and the action a_t is the next token o_t . The objective is defined over the generated sequence of length T :

$$\mathcal{L}_{PG}(\theta) = -\mathbb{E}_{q \sim \mathcal{D}, o \sim \pi_{\theta}} \left[\sum_{t=1}^T \log \pi_{\theta}(o_t | q, o_{<t}) \hat{A}_t \right],$$

where \hat{A}_t represents the advantage estimated at token step t .

In GRPO, the advantage is computed by normalizing rewards across a group of G outputs sampled for a single prompt. In the RLVR setting, the reward is assigned at the sequence level rather than per token, meaning all tokens within an output o share the same advantage estimate. Thus \hat{A}_t is constant across token steps t for a given question q and output o , and we denote it $\hat{A}_{q,o}$. We consider a binary verification reward $r_{\text{ver}} = 1$ for a correct final answer and $r_{\text{ver}} = 0$ otherwise.

Advantage computation. The verification reward follows a Bernoulli distribution: $r_{\text{ver}} \sim \text{Bernoulli}(p_q)$. The GRPO algorithm computes the advantage $\hat{A}_{q,o}$ by standardizing the reward:

$$\hat{A}_{q,o} = \frac{r_{\text{ver}} - \text{mean}(r_{\text{ver}})}{\text{std}(r_{\text{ver}})}.$$

Since $r_{\text{ver}} \sim \text{Bernoulli}(p_q)$, the moments are:

$$\text{mean}(r_{\text{ver}}) = p_q \quad \text{and} \quad \text{std}(r_{\text{ver}}) = \sqrt{p_q(1 - p_q)}.$$

Substituting these values, the advantage $\hat{A}_{q,o}$ takes on two distinct values depending on the correctness of the output¹:

¹This analysis extends to any reward of the form $r_{\text{total}} = r_{\text{ver}} + f(t)$, where $f(t)$ converges to a constant during training. See Appendix B for a formal proof.

- **Correct answer** (probability p_q): $\hat{A}_{q,o} = \frac{1 - p_q}{\sqrt{p_q(1 - p_q)}}$
- **Incorrect answer** (probability $1 - p_q$): $\hat{A}_{q,o} = \frac{-p_q}{\sqrt{p_q(1 - p_q)}}$

Zero-variance batches. When all G rollouts for a prompt q are simultaneously correct or simultaneously incorrect, every rollout receives the same reward, all advantages $\hat{A}_{q,o}$ are zero. The gradient contribution of the entire batch therefore vanishes and no parameter update occurs. The probability of this zero-variance event is

$$\mathbb{P}(\text{zero variance}) = p_q^G + (1 - p_q)^G, \quad (1)$$

which is minimized at $p_q = 1/2$ and approaches 1 as $p_q \rightarrow 0$ or $p_q \rightarrow 1$. Therefore, prompts near the extremes waste an entire group of rollouts with high probability, regardless of model capacity or training budget.

Gradient norm scaling. We have shown that substituting these advantage values into the policy gradient objective and separating the contributions of correct and incorrect outcomes gives

$$\begin{aligned} \|\nabla_{\theta} L_{PG}\| &= \sqrt{p_q(1 - p_q)} \left\| \mathbb{E} \left[\sum_{t=1}^T \nabla_{\theta} \log \pi_{\theta}(o_t | q, o_{<t}) \Big| r_{\text{ver}} = 1 \right] \right. \\ &\quad \left. - \mathbb{E} \left[\sum_{t=1}^T \nabla_{\theta} \log \pi_{\theta}(o_t | q, o_{<t}) \Big| r_{\text{ver}} = 0 \right] \right\| = \sqrt{p_q(1 - p_q)} \left\| \nabla_{\theta} \log \frac{p_q}{1 - p_q} \right\|. \quad (2) \end{aligned}$$

where the second equality is an exact identity expressing the gradient norm as the Bernoulli standard deviation $\sqrt{p_q(1 - p_q)}$ times the norm of the log-odds gradient $\nabla_{\theta} \log \frac{p_q(\theta)}{1 - p_q(\theta)}$, where $p_q = p_q(\theta)$ is the verification probability. The proof is given in Appendix C.

Exact identity and vanishing signal. Eq. (2) already reveals that the gradient norm scales as $\sqrt{p_q(1 - p_q)}$, which is maximized at $p_q = 1/2$. Under the additional assumption that the per-token gradient $\|\nabla_{\theta} \log \pi_{\theta}(o_t | q, o_{<t})\|$ is uniformly bounded by some constant B and the context length T is finite, this scaling translates into the upper bound

$$\|\nabla_{\theta} L_{PG}\| \leq 2BT \sqrt{p_q(1 - p_q)}, \quad (3)$$

where $p_q = p_q(\theta)$ is the verification probability at the current parameters. Eq. (3) shows that the gradient norm is structurally bounded by $\sqrt{p_q(1 - p_q)}$, with the constant $2BT$ uniform across all prompts at a fixed checkpoint. Therefore, as $p_q \rightarrow 0$ or $p_q \rightarrow 1$, the gradient norm $\|\nabla_{\theta} \mathcal{L}_{PG}\| \rightarrow 0$, leading to vanishing gradients. The formal proof is given in Appendix C.

Taken together, Eq. (1) and Eq. (3) give two independent reasons why prompts near $p_q \in \{0, 1\}$ are wasteful: they suppress the gradient magnitude and are overwhelmingly likely to produce zero-variance batches. Conversely, prompts near $p_q = 1/2$ minimize the probability of zero-variance batches Eq. (1) and saturate the structural upper bound on the gradient norm Eq. (3). This motivates the Goldilocks Teacher: select prompts at the edge of the model’s current solvability, where $\sqrt{p_q(1 - p_q)}$ is largest.

3 Joint Training Procedure

We now detail the overall training loop, illustrated in Figure 1. The process operates in a cycle that alternates between data selection, student optimization via GRPO, and continuous teacher refinement.

3.1 Data Selection Policy (Steps 1-2)

During the data selection phase, the Teacher samples a candidate pool, denoted as \mathcal{C} , consisting of $K_{\text{candidate}}$ examples drawn randomly from the dataset. For each candidate question $q \in \mathcal{C}$, the Teacher computes a predicted utility score $\hat{v}_q = f_{\phi}(q)$. To balance exploration and exploitation, the final training sample q^* is selected using an ϵ -greedy strategy (Algorithm 1):

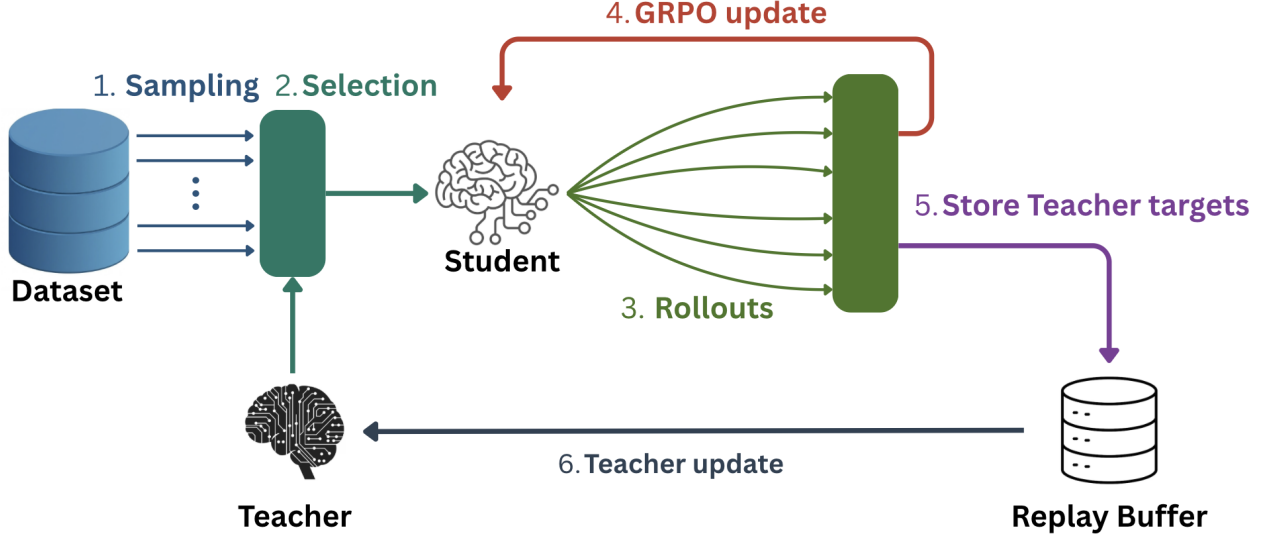


Figure 1: **Overview of the Goldilocks Framework.** The continuous Teacher-Student training loop.

- With probability ϵ , a question is selected uniformly at random from \mathcal{C} to ensure diverse data coverage.
- With probability $1 - \epsilon$, the question with the highest predicted utility is selected deterministically, i.e.,

$$q^* = \arg \max_{q \in \mathcal{C}} \hat{v}_q.$$

3.2 Student Rollouts and Optimization (Steps 3-4)

Once the prompt q^* is selected, the Student model generates a group of G rollouts, $\{o_1, \dots, o_G\}$. The verification reward r_{ver} is computed for each output, and the advantages are estimated using the group-relative normalization described in Section 2. Based on these advantages, the gradient is computed. To ensure optimization stability, gradients are accumulated over a batch of selected prompts before a parameter update is applied to the Student model.

3.3 Teacher Refinement (Steps 5-6)

The Teacher is trained online to predict the learning potential of specific prompts based on the Student’s real-time feedback. Following the Student’s rollouts for a question q , we calculate the empirical success rate \hat{p}_q as the fraction of correct solutions within the generated group. The regression target y_q is then set to the empirical standard deviation of the verification reward:

$$y_q = \sqrt{\hat{p}_q(1 - \hat{p}_q)}.$$

This tuple (q, y_q) is pushed into a replay buffer $\mathcal{D}_{\text{replay}}$ of capacity N_{replay} , which operates as a sliding window to retain the most recent interaction data.

The Teacher updates its parameters ϕ periodically as detailed in Algorithm 2. After every M_{update} samples processed by the Student, the Teacher undergoes a dedicated training phase lasting E_{teacher} epochs. During this phase, we iterate over the entire replay buffer $\mathcal{D}_{\text{replay}}$, processing the data in mini-batches \mathcal{B} to minimize the Mean Squared Error:

$$\mathcal{L}_{\mathcal{B}}(\phi) = \frac{1}{|\mathcal{B}|} \sum_{(q, y_q) \in \mathcal{B}} (f_{\phi}(q) - y_q)^2.$$

This objective ensures the Teacher continuously aligns its predictions with the Student’s capabilities.

4 Teacher and Student Architecture

4.1 Student

The Student model is initialized as a pretrained language model, parameterized by θ . It functions as the primary policy, denoted as $\pi_\theta(o | q)$, which maps an input question q to a generated output sequence o . This output typically consists of a reasoning chain followed by a final answer. The Student is fine-tuned via RL (specifically GRPO) to maximize the expected reward of its generated trajectories. Throughout the training process, the Student’s parameters are updated to improve the correctness of its reasoning, while serving as the source of feedback signals (success/failure) used to train the Teacher.

4.2 Teacher

The Teacher functions as a value predictor built upon a trainable language model backbone. For a given input question q , we extract the final layer embeddings and apply mean pooling to obtain a fixed-size vector representation. This vector is then passed through a linear projection layer. To strictly enforce the valid range of the standard deviation term (which lies between 0 and 0.5 for a Bernoulli variable), we apply a scaled sigmoid activation, i.e.,

$$f_\phi(q) = 0.5 \cdot \sigma(\mathbf{w}^T \cdot \text{MeanPool}(\text{Embed}(q)) + b),$$

where $f_\phi(q)$ represents the predicted utility of question q . The parameters ϕ encompass both the projection head and the pretrained language model, allowing the Teacher to learn deep semantic features relevant to difficulty estimation. For a detailed exploration of alternative teacher backbones and projection strategies, please refer to Appendix L.

5 Experiments and Results

To validate Goldilocks, we conduct a comprehensive evaluation using the OpenMathReasoning dataset [16], which comprises over 3 million chain-of-thought problems. Additional dataset details are in Appendix J. Following common practice in RL-based reasoning research [24, 3, 5], we focus on mathematical reasoning as our target domain. Given the substantial computational cost of GRPO experiments on this dataset (each requiring more than 1000 GPU hours), rather than extending evaluation across additional datasets, we prioritized longer training runs on this benchmark to ensure our method remains useful in extended training regimes; a detailed accounting of the total compute footprint and the rationale for prioritizing depth over benchmark breadth is provided in Appendix I. We train models using the GRPO algorithm across a diverse range of model families, including Qwen2.5-1.5B [33], Qwen3-4B [34], Phi-4-mini-instruct (a 4B model) [2], and Olmo2-1B [18]. All experiments were implemented using the TRL library [28].

5.1 Experimental Setup

For all experimental configurations, we employ the selected open-weight models as Student policies, optimizing them via GRPO with a fixed group size of $G = 16$. As discussed in the introduction, history-based and category-based curriculum methods are not applicable at this scale and cannot serve as direct baselines: history-based methods require multiple passes over each prompt to estimate per-instance difficulty, and category-based methods require difficulty labels the dataset does not provide. We therefore compare exclusively against vanilla GRPO under matched global batch size, hyperparameters, and effective compute, and rely on the training-dynamics analysis in Section 5.3 (zero-variance fraction, gradient norm, reward standard deviation) to characterize the source of the gain. We adopt a stratified strategy for Teacher instantiation: for compact architectures (Qwen2.5-1.5B and Olmo2-1B), the Teacher is initialized from the same base model as the Student. Conversely, for the larger 4B-parameter models (Phi-4-mini-instruct and Qwen3-4B), we utilize the Qwen3-1.7B [34] model as the Teacher to evaluate cross-model curriculum generation. Comprehensive implementation details are provided in Appendix K.

In all experiments, we utilized a fixed computational budget of 8 GPUs. For the GRPO baseline, all 8 GPUs were dedicated to the policy model. In contrast, the Goldilocks framework allocated 2 GPUs to the Teacher for dynamic data selection and 6 GPUs to the Student for training. Crucially, to isolate the efficacy of the curriculum strategy, we

Table 1: **Performance on OpenMathReasoning.** We compare the Pass@1 accuracy of the Goldilocks against the GRPO baseline. Models denoted with [†] employ a Qwen3-1.7B Teacher.

Model	Base Model	Baseline (GRPO)	Goldilocks (Ours)
Olmo2-1B	2.5%	11.7%	14.9%
Qwen2.5-1.5B	13.48%	30.6%	33.4%
Qwen3-4B [†]	12.4%	58.1%	59.7%
Phi-4-4B-Instruct [†]	25.4%	37.1%	41.0%

maintained identical global batch sizes and hyperparameters across both configurations. To ensure a fair comparison of computational cost, we normalize the training steps based on the effective resource allocation; specifically, we compare step n of the Goldilocks Student against step $\frac{8}{6}n$ of the baseline, strictly accounting for the difference in available compute for them. We justify this scheme in Appendix D.

5.2 Main Results

Table 1 presents the performance benchmarks on the validation set of the OpenMathReasoning. Detailed specifications for the training step counts and the step-balancing logic between Goldilocks and the baselines are provided in Appendix K.5.

For all reported validation accuracies, we average the last five validation steps to reduce statistical noise from both RL training and the evaluation itself, though accuracy plots are presented without denoising. All other training dynamics (e.g., student and teacher metrics) are smoothed using an Exponential Moving Average (EMA) with $\alpha = 0.9$.

Figure 2 depicts the validation accuracy curves throughout the optimization process, contrasting the baseline GRPO model Qwen2.5-1.5B with the Goldilocks Student Qwen2.5-1.5B and Teacher Qwen2.5-1.5B (see Appendix F for evaluations based on wall-clock time and token budget).

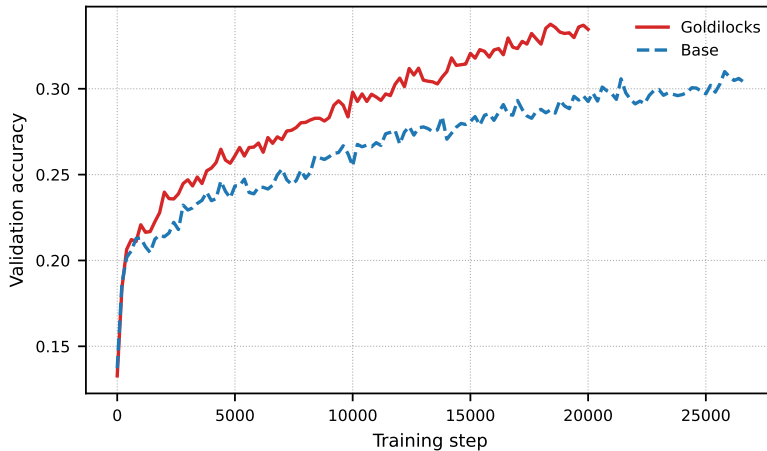


Figure 2: Evolution of validation accuracy over training steps.

5.3 Student Training Dynamics and Analysis

In this section, we examine the comparative training dynamics of the Goldilocks Student model relative to the GRPO baseline (for more figures see Appendix H). To understand the mechanism behind the improved performance, we first examine the evolution of the training success rate. Figure 3 compares the average r_{ver} and its standard deviation. The average reward of Goldilocks exhibits a steeper slope, indicating accelerated learning. Moreover, the vertical offset confirms our sampling objective: the Teacher actively prioritizes questions where p_q is closer to 0.5,

thereby maximizing the variance and learning signal, which is further confirmed by the consistently higher reward standard deviation shown in Figure 3b.

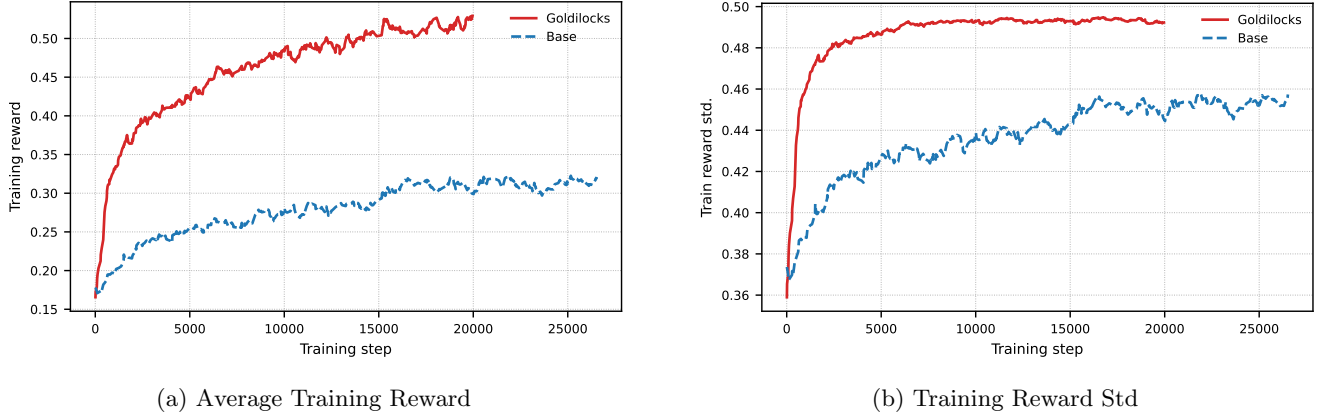


Figure 3: **Training Reward Dynamics.**

By prioritizing samples with higher uncertainty, Goldilocks significantly reduces the fraction of questions with zero variance (i.e., $p_q(1 - p_q) = 0$, leading to zero gradients during GRPO), as shown in Figure 4b, ensuring the optimizer rarely wastes computation on uninformative samples. Consequently, as shown in Figure 4a, Goldilocks maintains significantly larger gradient norms compared to the baseline, preventing optimization stagnation and ensuring more effective parameter updates per compute step. This empirically validates the theoretical result of Eq. (2), where we showed that the gradient norm scales linearly with $\sqrt{p_q(1 - p_q)}$.

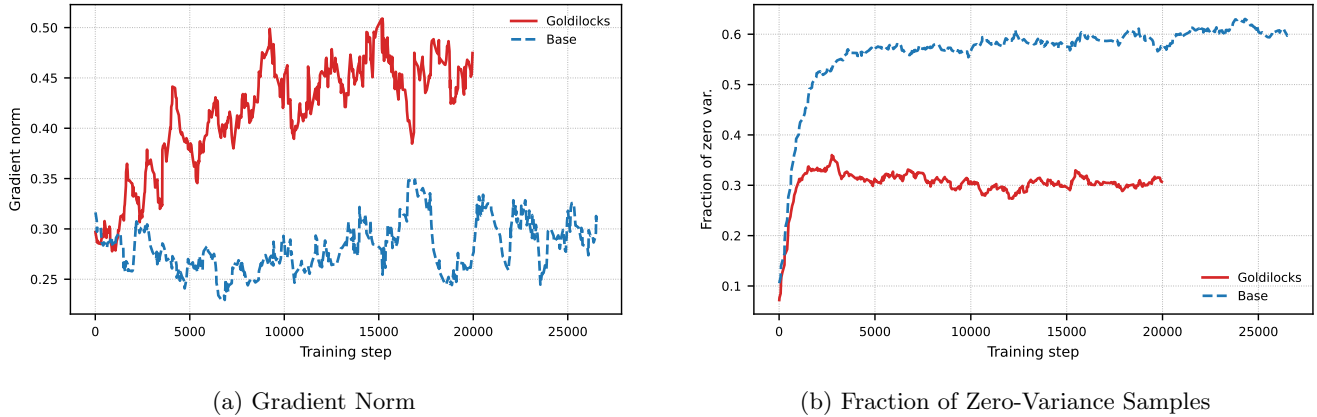


Figure 4: **Optimization Dynamics.**

5.4 Teacher Training Dynamics and Analysis

To validate the Teacher’s reliability, we track its Mean Absolute Error (MAE) on samples D_{new} not yet encountered in previous training steps, which serves as an online validation score:

$$\mathcal{L}_{MAE}(\phi) = \frac{1}{|D_{\text{new}}|} \sum_{(q, y_q) \in D_{\text{new}}} |f_{\phi}(q) - y_q|.$$

As shown in Figure 5a, this MAE decreases consistently over training, and the Teacher’s error on zero-variance samples remains lower, indicating that the Teacher generalizes well rather than memorizing the replay buffer. Beyond accuracy, Figure 5b tracks the mean (μ) and standard deviation (σ) of the Teacher’s predicted scores. The sustained σ confirms the Teacher continues to differentiate between difficulties, avoiding mode collapse, while the downward

trend in μ reflects the student’s growing mastery over the dataset, confirming that the Teacher dynamically adapts to the student’s evolving capabilities rather than remaining static.

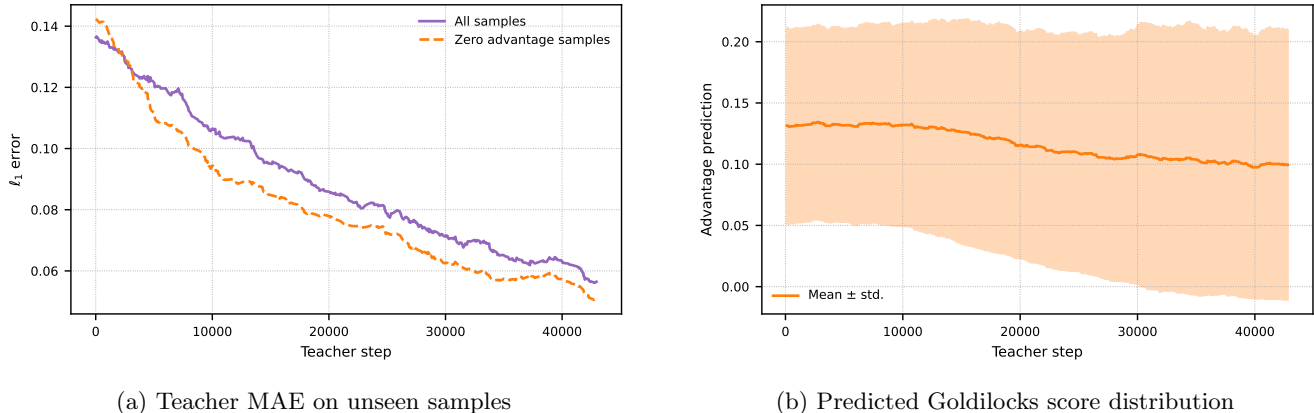


Figure 5: **Teacher Prediction Analysis.**

6 Ablation Study

To assess the versatility of Goldilocks, we conduct two independent ablation experiments using the Qwen2.5-1.5B model. These experiments isolate the impact of our curriculum strategy when paired with advanced loss formulations and explicit regularization terms. The detailed training plots for these experiments are provided in Appendix G.

Table 2: **Ablation Studies on Qwen2.5-1.5B.** Performance of Goldilocks and GRPO baseline across different settings.

Setting	Method	Param.	Acc. (%)
Standard GRPO	Baseline	–	27.6%
	Goldilocks	–	29.5%
DAPO Loss	Baseline	–	26.7%
	Goldilocks	–	28.0%
Entropy Reg.	Baseline	$\beta=0.0003$	27.4%
	Goldilocks	$\beta=0.0003$	29.1%

DAPO Loss. We evaluate the framework using the DAPO loss [37], which refines standard group-based optimization by enforcing mixed-quality batches. Unlike GRPO, DAPO explicitly constrains the sampled group $\{o_i\}_{i=1}^G$ to contain at least one correct and one incorrect solution (i.e., $0 < \text{correct count} < G$). The loss is computed by normalizing the clipped surrogate objective over the total token count of the group:

$$\mathcal{L}_{\text{DAPO}}(\theta) = \mathbb{E} \left[\frac{1}{\sum_{i=1}^G |o_i|} \sum_{i=1}^G \sum_{t=1}^{|o_i|} \min \left(r_{i,t}(\theta) \hat{A}_{i,t}, \text{clip} \left(r_{i,t}(\theta), 1 - \epsilon_{\text{low}}, 1 + \epsilon_{\text{high}} \right) \hat{A}_{i,t} \right) \right]$$

where $r_{i,t}(\theta)$ is the probability ratio $\frac{\pi_{\theta}(o_{i,t}|\cdot)}{\pi_{\theta_{\text{old}}}(o_{i,t}|\cdot)}$ and the advantage $\hat{A}_{i,t}$ is derived via group-wise normalization $\frac{R_i - \text{mean}(\{R\})}{\text{std}(\{R\})}$. We train both the baseline and the Goldilocks student using this formulation while keeping all other hyperparameters constant. As shown in Table 2, Goldilocks retains its performance advantage, demonstrating that our curriculum-based data selection provides benefits orthogonal to the specific alignment loss employed.

Entropy Regularization. In a separate experiment, we investigate the effect of entropy regularization on the standard GRPO objective. The policy entropy $\mathcal{H}(\pi_\theta(\cdot|x))$ quantifies the diversity of the generated reasoning paths. We introduce an entropy bonus coefficient β to the loss function:

$$\mathcal{L}_{total} = \mathcal{L}_{GRPO} + \beta \mathbb{E}_{x \sim \mathcal{D}}[\mathcal{H}(\pi_\theta(\cdot|x))]. \quad (4)$$

Maximizing this term prevents premature convergence by encouraging the model to explore a wider range of solution paths. We compare the baseline against Goldilocks with a fixed coefficient of $\beta = 0.0003$. The results, presented in the bottom section of Table 2, indicate that even when both models are forced to explore via regularization, Goldilocks maintains its performance advantage.

7 Related Works

Reasoning, Scratchpads, and Chain-of-Thought. It is widely established that success on challenging reasoning problems requires models to perform intermediate computations rather than deducting final answers directly. Early work by Nye et al. [17] demonstrated that supervised training with “scratchpads” significantly improves performance on tasks like polynomial evaluation and code execution. The study by Wei et al. [30] formalized this as Chain-of-Thought (CoT) prompting, showing that language models can generate reasoning traces via in-context demonstrations without explicit training, while Kojima et al. [12] extended this capability to the zero-shot setting. Theoretically, Abbe et al. [1] put forward the notion of globality degree of a task as a hardness measure, showing that scratchpads can make learning more efficient by breaking the globality of a task. Furthermore, to improve robustness, Gao et al. [8] proposed training on mathematical abstractions of reasoning traces rather than natural language.

RL for Reasoning. Several studies have highlighted the difficulty of applying RL to structured reasoning tasks due to the complexity of the output space [27, 14]. Standard policy gradient approaches such as PPO [23, 20] and, more recently, GRPO [24] have been adapted to optimize CoT generation using outcome-based verification rewards. A central challenge in this domain is the sparsity of rewards; models must navigate vast search spaces with binary feedback (correct/incorrect), making sample efficiency a significant bottleneck [38]. Consequently, methods that can prioritize high-signal training data are essential for scaling these techniques.

Curriculum Learning in Reasoning. Curriculum learning addresses data inefficiency by organizing training samples to optimize the learning trajectory. Recent strategies focus on identifying the “frontier” of model capability, building on early Teacher-Student frameworks [15]. Several methods stabilize training by targeting a desired success rate: Qu et al. [22] model question difficulty via a Beta distribution to select samples near a target accuracy γ^* , while Shen et al. [25] employ Thompson sampling for similar objectives. Others maximize the gradient signal directly—Chen et al. [5] prioritize samples with high absolute advantage ($|\hat{A}_q|$) using exponential moving averages, and Li et al. [13] allocate rollout budgets to avoid trivial samples yielding zero gradients. A complementary line filters samples *after* generation: Wang et al. [29] and Xiong et al. [32] perform rollouts and skip the policy update on uninformative ones, though the dominant generation cost is still incurred. Closer to our setting, Gu et al. [9] replace history-based heuristics with a bandit-based co-adaptive curriculum, but their formulation is restricted to small-scale datasets. Overall, none of these methods scale to large dataset regimes. Scaffolding approaches [3, 31] instead provide partial solutions that are progressively shortened over training.

8 Limitation and Future Work

In this work, we introduced Goldilocks, a teacher-driven framework that dynamically constructs a training curriculum for reasoning models. While traditional curriculum strategies often operate under significant constraints—relying on history-dependent metrics that require prior interaction with specific samples, or necessitating restrictive auxiliary information like pre-categorized datasets—our approach overcomes these limitations. The Goldilocks Teacher possesses the unique capability to predict the learning potential of unseen questions directly, enabling it to generalize to novel data streams that neither the Student nor the Teacher has previously encountered.

This zero-shot difficulty estimation allows the framework to filter out uninformative samples before the Student expends computational resources on them, significantly accelerating training convergence. Looking forward, this

paradigm holds promise for several high-impact directions. First, the variance-aware selection policy could be adapted to other complex domains, such as code generation or theorem proving. Second, and perhaps most critically, this methodology could be applied to large-scale pretraining, where dynamically filtering trillion-token corpora based on predicted utility could drastically reduce training costs and improve model quality.

References

- [1] Emmanuel Abbe, Samy Bengio, Aryo Lotfi, Colin Sandon, and Omid Saremi. How far can transformers reason? the globality barrier and inductive scratchpad. *Advances in Neural Information Processing Systems*, 37: 27850–27895, 2024.
- [2] Marah Abdin, Jyoti Aneja, Harkirat Behl, Sébastien Bubeck, Ronen Eldan, Suriya Gunasekar, Michael Harrison, Russell J Hewett, Mojan Javaheripi, Piero Kauffmann, et al. Phi-4 technical report. *arXiv preprint arXiv:2412.08905*, 2024.
- [3] Mohammad Hossein Amani, Aryo Lotfi, Nicolas Mario Baldwin, Samy Bengio, Mehrdad Farajtabar, Emmanuel Abbe, and Robert West. Rl for reasoning by adaptively revealing rationales. *arXiv preprint arXiv:2506.18110*, 2025.
- [4] Yoshua Bengio, Jérôme Louradour, Ronan Collobert, and Jason Weston. Curriculum learning. In *Proceedings of the 26th annual international conference on machine learning*, pages 41–48, 2009.
- [5] Xiaoyin Chen, Jiarui Lu, Minsu Kim, Dinghuai Zhang, Jian Tang, Alexandre Piché, Nicolas Gontier, Yoshua Bengio, and Ehsan Kamaloo. Self-evolving curriculum for llm reasoning. *arXiv preprint arXiv:2505.14970*, 2025.
- [6] Karl Cobbe, Vineet Kosaraju, Mohammad Bavarian, Mark Chen, Heewoo Jun, Lukasz Kaiser, Matthias Plappert, Jerry Tworek, Jacob Hilton, Reiichiro Nakano, Christopher Hesse, and John Schulman. Training verifiers to solve math word problems. *arXiv preprint arXiv:2110.14168*, 2021.
- [7] DeepSeek-AI, Dayiheng Liu, et al. Deepseek-r1: Incentivizing reasoning capability in llms via reinforcement learning. *arXiv preprint arXiv:2501.12948*, 2025.
- [8] Silin Gao, Antoine Bosselut, Samy Bengio, and Emmanuel Abbe. Abstral: Augmenting llms’ reasoning by reinforcing abstract thinking. *arXiv preprint arXiv:2406.11228*, 2024.
- [9] Zhengyao Gu, Jonathan Light, Raul Astudillo, Ziyu Ye, Langzhou He, Henry Peng Zou, Wei Cheng, Santiago Paternain, Philip S Yu, and Yisong Yue. Actor-curator: Co-adaptive curriculum learning via policy-improvement bandits for rl post-training. *arXiv preprint arXiv:2602.20532*, 2026.
- [10] Zhenyu Hou, Xin Lv, Rui Lu, Jiajie Zhang, Yujiang Li, Zijun Yao, Juanzi Li, Jie Tang, and Yuxiao Dong. T1: Advancing language model reasoning through reinforcement learning and inference scaling. *arXiv preprint arXiv:2501.11651*, 2025.
- [11] Devvrit Khatri, Lovish Madaan, Rishabh Tiwari, Rachit Bansal, Sai Surya Duvvuri, Manzil Zaheer, Inderjit S Dhillon, David Brandfonbrener, and Rishabh Agarwal. The art of scaling reinforcement learning compute for llms. *arXiv preprint arXiv:2510.13786*, 2025.
- [12] Takeshi Kojima, Shixiang Shane Gu, Machel Reid, Yutaka Matsuo, and Yusuke Iwasawa. Large language models are zero-shot reasoners. In *Advances in Neural Information Processing Systems*, 2022.
- [13] Ziniu Li, Congliang Chen, Tianyun Yang, Tian Ding, Ruoyu Sun, Ge Zhang, Wenhao Huang, and Zhi-Quan Luo. Knapsack rl: Unlocking exploration of llms via optimizing budget allocation. *arXiv preprint arXiv:2509.25849*, 2025.
- [14] Hunter Lightman, Vineet Kosaraju, Yura Burda, Harri Edwards, Bowen Baker, Teddy Lee, et al. Let’s verify step by step. *arXiv preprint arXiv:2305.20050*, 2023.

- [15] Tabet Matiisen, Avital Oliver, Taco Cohen, and John Schulman. Teacher–student curriculum learning. *IEEE transactions on neural networks and learning systems*, 31(9):3732–3740, 2019.
- [16] Ivan Moshkov, Darragh Hanley, Ivan Sorokin, Shubham Toshniwal, Christof Henkel, Benedikt Schifferer, Wei Du, and Igor Gitman. Aimo-2 winning solution: Building state-of-the-art mathematical reasoning models with openmathreasoning dataset. *arXiv preprint arXiv:2504.16891*, 2025.
- [17] Maxwell Nye, Anders Johan Andreassen, Guy Gur-Ari, Henryk Michalewski, Jacob Austin, David Bieber, David Dohan, Aitor Lewkowycz, Maarten Bosma, David Luan, et al. Show your work: Scratchpads for intermediate computation with language models. *ICLR 2022*, 2021.
- [18] Team OLMo, Pete Walsh, Luca Soldaini, Dirk Groeneveld, Kyle Lo, Shane Arora, Akshita Bhagia, Yuling Gu, Shengyi Huang, Matt Jordan, et al. 2 olmo 2 furious. *arXiv preprint arXiv:2501.00656*, 2024.
- [19] OpenAI. Learning to reason with llms. <https://openai.com/index/learning-to-reason-with-llms/>, 2024. Accessed: 2025-01-20.
- [20] Long Ouyang, Jeffrey Wu, Xu Jiang, Diogo Almeida, Carroll Wainwright, Pamela Mishkin, et al. Training language models to follow instructions with human feedback. In *Advances in Neural Information Processing Systems*, volume 35, pages 27730–27744, 2022.
- [21] Shubham Parashar, Shurui Gui, Xiner Li, Hongyi Ling, Sushil Vemuri, Blake Olson, Eric Li, Yu Zhang, James Caverlee, Dileep Kalathil, et al. Curriculum reinforcement learning from easy to hard tasks improves llm reasoning. *arXiv preprint arXiv:2506.06632*, 2025.
- [22] Yun Qu, Qi Wang, Yixiu Mao, Vincent Tao Hu, Björn Ommer, and Xiangyang Ji. Can prompt difficulty be online predicted for accelerating rl finetuning of reasoning models? *arXiv preprint arXiv:2507.04632*, 2025.
- [23] John Schulman, Filip Wolski, Prafulla Dhariwal, Alec Radford, and Oleg Klimov. Proximal policy optimization algorithms. *arXiv preprint arXiv:1707.06347*, 2017.
- [24] Zhihong Shao, Peiyi Wang, Qihao Zhu, Runxin Xu, Alan Song, Mingchuan Xiao, et al. Deepseekmath: Pushing the limits of mathematical reasoning in open language models. *arXiv preprint arXiv:2402.03300*, 2024. Introduces GRPO.
- [25] Qianli Shen, Daoyuan Chen, Yilun Huang, Zhenqing Ling, Yaliang Li, Bolin Ding, and Jingren Zhou. Bots: A unified framework for bayesian online task selection in llm reinforcement finetuning. *arXiv preprint arXiv:2510.26374*, 2025.
- [26] Charlie Snell, Jaehoon Lee, Kelley Xu, and Aviral Kumar. Scaling llm test-time compute optimally can be more effective than scaling llm parameters. *arXiv preprint arXiv:2408.03314*, 2024.
- [27] Jonathan Uesato, Nate Kushman, Ram Kumar, Francis Song, Noah Siegel, Lisa Wang, et al. Solving math word problems with process- and outcome-based feedback. In *arXiv preprint arXiv:2211.14275*, 2022.
- [28] Leandro von Werra, Younes Belkada, Lewis Tunstall, Edward Beeching, Tristan Thrush, Nathan Lambert, Shengyi Huang, Kashif Rasul, and Quentin Gallouédec. TRL: Transformers Reinforcement Learning, 2020. URL <https://github.com/huggingface/trl>.
- [29] Zhenting Wang, Guofeng Cui, Yu-Jhe Li, Kun Wan, and Wentian Zhao. Dump: Automated distribution-level curriculum learning for rl-based llm post-training. *arXiv preprint arXiv:2504.09710*, 2025.
- [30] Jason Wei, Xuezhi Wang, Dale Schuurmans, Maarten Bosma, Ed Chi, Quoc Le, and Denny Zhou. Chain-of-thought prompting elicits reasoning in large language models. In *Advances in Neural Information Processing Systems*, 2022.
- [31] Zhiheng Xi, Wenxiang Chen, Boyang Hong, Senjie Jin, Rui Zheng, Wei He, Yiwen Ding, Shichun Liu, Xin Guo, Junzhe Wang, et al. Training large language models for reasoning through reverse curriculum reinforcement learning. *arXiv preprint arXiv:2402.05808*, 2024.

- [32] Wei Xiong, Chenlu Ye, Baohao Liao, Hanze Dong, Xinxing Xu, Christof Monz, Jiang Bian, Nan Jiang, and Tong Zhang. Reinforce-ada: An adaptive sampling framework under non-linear rl objectives. *arXiv preprint arXiv:2510.04996*, 2025.
- [33] An Yang, Baosong Yang, Binyuan Hui, Bo Zheng, Bowen Yu, Chang Zhou, Chengpeng Li, Chengyuan Li, Dayiheng Liu, Fei Huang, Guanting Dong, Haoran Wei, Huan Lin, Jialong Tang, Jialin Wang, Jian Yang, Jianhong Tu, Jianwei Zhang, Jianxin Yang, Jiayi Yang, Jingren Zhou, Jinze Bai, Jinzheng He, Junyang Lin, Kai Dang, Keming Lu, Keqin Bao, Kexin Yang, Le Yu, Mei Li, Mingfeng Xue, Pei Zhang, Qin Zhu, Rui Men, Runxin Xu, Tianhao Li, Tianyu Liu, Wang Fan, Wenbin Ge, Xiaodong Deng, Xiaohuan Zhou, Xingzhang Ren, Xinyu Zhang, Xinyuan Li, Yang Fan, Yang Tan, Yu Wan, Yuze Gao, Yuqiang Xie, Zekun Wang, Zengmao Wang, Zhihao Xiang, Zhitang Li, Zhiyuan Gao, Zhiyuan Xu, and Zick Ye. Qwen2.5 technical report. *arXiv preprint arXiv:2412.15115*, 2024. URL <https://arxiv.org/abs/2412.15115>.
- [34] An Yang, Anfeng Li, Baosong Yang, Beichen Zhang, Binyuan Hui, Bo Zheng, Bowen Yu, Chang Gao, Chengen Huang, Chenxu Lv, et al. Qwen3 technical report. *arXiv preprint arXiv:2505.09388*, 2025.
- [35] Huahui Yi, Kun Wang, Qiankun Li, Miao Yu, Liang Lin, Gongli Xi, Hao Wu, Xuming Hu, Kang Li, and Yang Liu. Safer-vlm: Toward safety-aware fine-grained reasoning in multimodal models. *arXiv preprint arXiv:2510.06871*, 2025.
- [36] Fei Yu, Anningzhe Gao, and Benyou Wang. Ovm, outcome-supervised value models for planning in mathematical reasoning. *arXiv preprint arXiv:2311.09724*, 2023.
- [37] Qiyang Yu, Zheng Zhang, Ruofei Zhu, Yufeng Yuan, Xiaochen Zuo, Yu Yue, Weinan Dai, Tiantian Fan, Gaohong Liu, Lingjun Liu, et al. Dapo: An open-source llm reinforcement learning system at scale. *arXiv preprint arXiv:2503.14476*, 2025.
- [38] Eric Zelikman, Yuhuai Wu, Jesse Mu, and Noah Goodman. Star: Bootstrapping reasoning with reasoning. In *Advances in Neural Information Processing Systems*, volume 35, pages 15476–15488, 2022.

A Algorithms

Algorithm 1 Goldilocks Teacher: Data Selection Policy

```

1: Input: Dataset  $\mathcal{D}$ , Teacher Model  $f_\phi$ , Candidate Size  $K$ , Exploration  $\epsilon$ .
2: Output: Selected question  $q^*$ .
3: function SelectQuery( $\phi, \mathcal{D}$ )
4:    $\mathcal{C} \leftarrow$  Sample  $K$  random indices from  $\mathcal{D}$ 
5:    $\mathcal{V} \leftarrow \emptyset$ 
6:   for each candidate  $q \in \mathcal{C}$  do
7:      $\hat{v}_q \leftarrow f_\phi(q)$  {Predict learning utility}
8:      $\mathcal{V} \leftarrow \mathcal{V} \cup \{\hat{v}_q\}$ 
9:   end for
10:   $r \sim \text{Uniform}(0, 1)$ 
11:  if  $r < \epsilon$  then
12:     $q^* \leftarrow \text{Uniform}(\mathcal{C})$  {Ensure coverage ( $\epsilon$ -greedy)}
13:  else
14:     $q^* \leftarrow \arg \max_{q \in \mathcal{C}} \hat{v}_q$  {Greedy maximization}
15:  end if
16:  return  $q^*$ 
17: end function

```

Algorithm 2 Goldilocks Teacher: Online Refinement

```

1: Input: Question  $q$ , Rollouts  $\{o_1, \dots, o_G\}$ , Teacher Model  $f_\phi$ , Replay Buffer  $\mathcal{D}_{\text{replay}}$ , Capacity  $N_{\text{replay}}$ .
2: function UpdateTeacher( $q, \{o_i\}_{i=1}^G$ )
3:   $\hat{p}_q \leftarrow \frac{1}{G} \sum_{i=1}^G \mathbb{I}(o_i \text{ is correct})$  {Empirical success rate}
4:   $y_q \leftarrow \sqrt{\hat{p}_q(1 - \hat{p}_q)}$  {Compute target utility}
5:  Push  $(q, y_q)$  to  $\mathcal{D}_{\text{replay}}$ 
6:  if  $|\mathcal{D}_{\text{replay}}| > N_{\text{replay}}$  then
7:    Remove oldest sample from  $\mathcal{D}_{\text{replay}}$  {Sliding window}
8:  end if
9:  {Periodic Update Trigger (Step 6)}
10: if Update Condition Met then
11:   Shuffle  $\mathcal{D}_{\text{replay}}$  and create batches  $\mathcal{B}$ 
12:   for epoch 1 to  $E_{\text{teacher}}$  do
13:     for batch  $B \in \mathcal{B}$  do
14:        $\mathcal{L} \leftarrow \frac{1}{|B|} \sum_{(q,y) \in B} (f_\phi(q) - y)^2$ 
15:        $\phi \leftarrow \phi - \eta \nabla_\phi \mathcal{L}$  {Gradient descent step}
16:     end for
17:   end for
18: end if
19: end function

```

B Generalization to Composite Rewards

Assumption 1 (Convergence of auxiliary reward). *Let $r_{\text{total}} = r_{\text{ver}} + f(t)$, where $f(t)$ is any reward component depending on training step t . There exists an iteration threshold $N \in \mathbb{N}$ such that for all $t \geq N$, $f(t) = C$ for some constant $C \in \mathbb{R}$.*

Proposition 1. *Under Assumption 1, for sufficiently large t , the GRPO advantage computed from r_{total} is identical to that computed from r_{ver} alone.*

Proof. For $t \geq N$, we have $r_{\text{total}} = r_{\text{ver}} + C$. Since $r_{\text{ver}} \sim \text{Bernoulli}(p_q)$:

$$\text{mean}(r_{\text{total}}) = p_q + C, \quad \text{std}(r_{\text{total}}) = \sqrt{p_q(1 - p_q)}.$$

The advantage is:

$$\begin{aligned} \hat{A}_q &= \frac{r_{\text{total}} - \text{mean}(r_{\text{total}})}{\text{std}(r_{\text{total}})} \\ &= \frac{(r_{\text{ver}} + C) - (p_q + C)}{\sqrt{p_q(1 - p_q)}} \\ &= \frac{r_{\text{ver}} - p_q}{\sqrt{p_q(1 - p_q)}}, \end{aligned}$$

which is identical to the advantage computed from r_{ver} alone. \square

C Proofs for GRPO with Verifiable Reward

In this appendix, we provide the formal derivations and proofs for the policy gradient properties under the GRPO framework with binary verifiable rewards. First, we derive the decomposition of the policy gradient norm. Then, we use this decomposition to prove the exact scaling identity and the structural upper bound of the gradient signal.

C.1 Derivation of the Gradient Norm Decomposition

Recall that the gradient of the standard policy objective for a fixed prompt q is the expected product of the trajectory score $S_\theta(o)$ and the sequence-level advantage $\hat{A}_{q,o}$:

$$\nabla_\theta \mathcal{L}_{\text{PG}} = -\mathbb{E}_{o \sim \pi_\theta} \left[S_\theta(o) \hat{A}_{q,o} \right], \quad (5)$$

where the trajectory score is $S_\theta(o) = \sum_{t=1}^T \nabla_\theta \log \pi_\theta(o_t \mid q, o_{<t})$.

As established in Section 2, the advantage is the standardized binary reward. Since $r_{\text{ver}} \sim \text{Bernoulli}(p_q)$, we substitute the advantage:

$$\hat{A}_{q,o} = \frac{r_{\text{ver}} - p_q}{\sqrt{p_q(1 - p_q)}}$$

Plugging this into the gradient expectation yields:

$$\nabla_\theta \mathcal{L}_{\text{PG}} = -\mathbb{E}_{o \sim \pi_\theta} \left[S_\theta(o) \frac{r_{\text{ver}} - p_q}{\sqrt{p_q(1 - p_q)}} \right]$$

Because $r_{\text{ver}} \in \{0, 1\}$, we apply the law of total expectation to split this into two conditional branches weighted by their respective probabilities, p_q and $(1 - p_q)$:

$$\nabla_\theta \mathcal{L}_{\text{PG}} = - \left(p_q \mathbb{E} \left[S_\theta(o) \frac{1 - p_q}{\sqrt{p_q(1 - p_q)}} \mid r_{\text{ver}} = 1 \right] + (1 - p_q) \mathbb{E} \left[S_\theta(o) \frac{0 - p_q}{\sqrt{p_q(1 - p_q)}} \mid r_{\text{ver}} = 0 \right] \right)$$

Since p_q is constant with respect to the inner expectation, we can factor the scalars out. Notice that the coefficients for both terms evaluate to the exact same magnitude:

$$\frac{p_q(1-p_q)}{\sqrt{p_q(1-p_q)}} = \sqrt{p_q(1-p_q)}$$

Substituting this simplified coefficient back into the expression gives:

$$\nabla_{\theta} \mathcal{L}_{PG} = - \left(\sqrt{p_q(1-p_q)} \mathbb{E}[S_{\theta}(o) \mid r_{\text{ver}} = 1] - \sqrt{p_q(1-p_q)} \mathbb{E}[S_{\theta}(o) \mid r_{\text{ver}} = 0] \right)$$

Factoring out the $\sqrt{p_q(1-p_q)}$ scalar and taking the norm of both sides yields the gradient norm decomposition:

$$\|\nabla_{\theta} \mathcal{L}_{PG}\| = \sqrt{p_q(1-p_q)} \left\| \mathbb{E}[S_{\theta}(o) \mid r_{\text{ver}} = 1] - \mathbb{E}[S_{\theta}(o) \mid r_{\text{ver}} = 0] \right\| \quad (6)$$

C.2 Proof of the Exact Scaling Identity and Upper Bound

Theorem 1 (Exact scaling and upper bound of the policy-gradient norm for binary verification rewards). *Fix a prompt q , and let $p_q(\theta) = \Pr_{\pi_{\theta}}(r_{\text{ver}} = 1 \mid q)$. Given the policy-gradient norm decomposition in Eq. (6), then for every $p_q \in (0, 1)$, the exact gradient norm is given by:*

$$\|\nabla_{\theta} \mathcal{L}_{PG}\| = \sqrt{p_q(1-p_q)} \left\| \nabla_{\theta} \log \frac{p_q}{1-p_q} \right\|$$

Furthermore, if the per-token score is bounded such that $\|\nabla_{\theta} \log \pi_{\theta}(o_t \mid q, o_{<t})\| \leq B$, then the gradient norm satisfies the upper bound:

$$\|\nabla_{\theta} \mathcal{L}_{PG}\| \leq 2BT \sqrt{p_q(1-p_q)}$$

Proof. By definition, the expected reward is:

$$p_q(\theta) = \mathbb{E}_{o \sim \pi_{\theta}(\cdot \mid q)}[r_{\text{ver}}(o)]$$

Using the likelihood-ratio identity (REINFORCE trick), the gradient of this probability is:

$$\nabla_{\theta} p_q = \nabla_{\theta} \mathbb{E}_{\pi_{\theta}}[r_{\text{ver}}(o)] = \mathbb{E}_{\pi_{\theta}}[r_{\text{ver}}(o) S_{\theta}(o)]$$

Since $r_{\text{ver}} \in \{0, 1\}$, this expectation simplifies to:

$$\nabla_{\theta} p_q = p_q \mathbb{E}[S_{\theta}(o) \mid r_{\text{ver}} = 1]$$

Therefore, isolating the conditional expectation gives:

$$\mathbb{E}[S_{\theta}(o) \mid r_{\text{ver}} = 1] = \frac{\nabla_{\theta} p_q}{p_q} \quad (7)$$

Next, since π_{θ} is a normalized probability distribution, the expected score is zero:

$$\mathbb{E}_{\pi_{\theta}}[S_{\theta}(o)] = \mathbb{E}_{\pi_{\theta}}[\nabla_{\theta} \log \pi_{\theta}(o \mid q)] = \nabla_{\theta} \int \pi_{\theta}(o \mid q) do = \nabla_{\theta} 1 = 0$$

By the law of total expectation, conditioning on the binary reward yields:

$$\mathbb{E}[S_{\theta}(o)] = p_q \mathbb{E}[S_{\theta}(o) \mid r_{\text{ver}} = 1] + (1-p_q) \mathbb{E}[S_{\theta}(o) \mid r_{\text{ver}} = 0]$$

Setting the left-hand side to zero and substituting our previous result in Eq. (7) for the successful trajectories gives:

$$\nabla_{\theta} p_q + (1-p_q) \mathbb{E}[S_{\theta}(o) \mid r_{\text{ver}} = 0] = 0$$

Solving for the conditional expectation of failed trajectories yields:

$$\mathbb{E}[S_\theta(o) \mid r_{\text{ver}} = 0] = -\frac{\nabla_\theta p_q}{1 - p_q} \quad (8)$$

Now substitute Eq. (7) and Eq. (8) back into the gradient decomposition from Eq. (6):

$$\begin{aligned} \|\nabla_\theta \mathcal{L}_{\text{PG}}\| &= \sqrt{p_q(1 - p_q)} \left\| \frac{\nabla_\theta p_q}{p_q} - \left(-\frac{\nabla_\theta p_q}{1 - p_q} \right) \right\| \\ &= \sqrt{p_q(1 - p_q)} \left\| \frac{\nabla_\theta p_q}{p_q} + \frac{\nabla_\theta p_q}{1 - p_q} \right\| \\ &= \sqrt{p_q(1 - p_q)} \left\| \frac{\nabla_\theta p_q}{p_q(1 - p_q)} \right\| \\ &= \frac{\|\nabla_\theta p_q\|}{\sqrt{p_q(1 - p_q)}} \end{aligned}$$

This proves the exact norm identity.

To prove the log-odds equivalence, observe that by the chain rule:

$$\nabla_\theta \log \frac{p_q}{1 - p_q} = \frac{1}{\frac{p_q}{1 - p_q}} \cdot \frac{\nabla_\theta p_q(1 - p_q) - p_q(-\nabla_\theta p_q)}{(1 - p_q)^2} = \frac{\nabla_\theta p_q}{p_q} + \frac{\nabla_\theta p_q}{1 - p_q} = \frac{\nabla_\theta p_q}{p_q(1 - p_q)}$$

Therefore, multiplying by $\sqrt{p_q(1 - p_q)}$ establishes the equivalence:

$$\sqrt{p_q(1 - p_q)} \left\| \nabla_\theta \log \frac{p_q}{1 - p_q} \right\| = \frac{\|\nabla_\theta p_q\|}{\sqrt{p_q(1 - p_q)}} = \|\nabla_\theta \mathcal{L}_{\text{PG}}\|$$

Finally, to establish the upper bound, we assume that the per-token score is bounded by B :

$$\|\nabla_\theta \log \pi_\theta(o_t \mid q, o_{<t})\| \leq B$$

By the triangle inequality, the total trajectory score $S_\theta(o)$ is bounded by:

$$\|S_\theta(o)\| = \left\| \sum_{t=1}^T \nabla_\theta \log \pi_\theta(o_t \mid q, o_{<t}) \right\| \leq \sum_{t=1}^T \|\nabla_\theta \log \pi_\theta(o_t \mid q, o_{<t})\| \leq BT$$

Because the norm of the random variable is uniformly bounded by BT , its conditional expectations are also uniformly bounded by BT :

$$\|\mathbb{E}[S_\theta(o) \mid r_{\text{ver}} = 1]\| \leq BT \quad \text{and} \quad \|\mathbb{E}[S_\theta(o) \mid r_{\text{ver}} = 0]\| \leq BT$$

Applying the triangle inequality to the initial gradient norm decomposition from Eq. (6):

$$\begin{aligned} \|\nabla_\theta \mathcal{L}_{\text{PG}}\| &= \sqrt{p_q(1 - p_q)} \|\mathbb{E}[S_\theta(o) \mid r_{\text{ver}} = 1] - \mathbb{E}[S_\theta(o) \mid r_{\text{ver}} = 0]\| \\ &\leq \sqrt{p_q(1 - p_q)} \left(\|\mathbb{E}[S_\theta(o) \mid r_{\text{ver}} = 1]\| + \|\mathbb{E}[S_\theta(o) \mid r_{\text{ver}} = 0]\| \right) \\ &\leq \sqrt{p_q(1 - p_q)} (BT + BT) \\ &= 2BT \sqrt{p_q(1 - p_q)} \end{aligned}$$

This confirms both the exact scaling behavior and the uniform structural upper bound, completing the proof. \square

D Compute Allocation and Step Normalization

In this section, we want to clarify why Goldilocks and the GRPO baseline are compared at different step counts, and why this normalization make the comparison fair.

The 2 GPUs allocated to the Teacher are responsible for two concurrent operations: scoring candidate prompts on demand whenever the Student requests a new sample, and periodically fine-tuning the Teacher’s parameters on the replay buffer every M_{update} samples (Sections 3.1 and 3.3). Because the Student now runs on 6 GPUs instead of 8, we increase its gradient accumulation steps from 9 to 12 (for small models) and from 12 to 16 (for 4B models) so that the global batch size of 288 is preserved across both configurations (Appendix K.1). The consequence is that each Goldilocks Student step takes $8/6 \approx 1.33\times$ longer than a baseline step, since it accumulates over more micro-batches on fewer devices. Equivalently, at any matched step count, the baseline has performed 33% more Student-side work than Goldilocks.

Comparing the two methods at the same step count would therefore hand the baseline a substantial compute advantage on the policy itself, masking part of the curriculum’s contribution. To eliminate this asymmetry, we compare Goldilocks at step n against the baseline at step $\frac{8}{6}n$, so that both methods are evaluated after the same amount of Student-side computation. Concretely, each baseline run is extended to $\frac{4}{3}\times$ the step count of its Goldilocks counterpart, with the exact per-model step counts reported in Appendix K.5.

With this normalization, the Teacher’s compute overhead is no longer a confound. The total GPU budget is fixed at 8 for both methods, and the Student-side computation is equalized at every comparison point: the 2 GPUs Goldilocks spends on the Teacher are 2 GPUs it does not get to spend on the Student, and the step-normalization ensures the baseline is not implicitly rewarded for that difference.

E Experiment with Different Seeds

To ensure the statistical reliability of our findings, we conducted additional experiments evaluating the Qwen2.5-1.5B model across five independent random seeds. While we recognize the value of multi-seed evaluations across all evaluated models, the computational cost of these experiments is exceptionally high—a single training run requires over 1,000 GPU hours. Consequently, performing a comprehensive multi-seed analysis for every model is computationally infeasible. To robustly demonstrate statistical reliability within our compute constraints, we selected the Qwen2.5-1.5B model as a representative test case.

As summarized in Table 3, the results demonstrate a consistent and statistically significant advantage for the Goldilocks method over the standard GRPO baseline. Specifically, after 20,000 iterations, the Goldilocks method achieves a mean score of 33.0 (sample standard deviation of 0.54). In contrast, the standard GRPO baseline plateaus at a lower mean score of 30.2 (sample standard deviation of 0.48), even after an extended training run of 26,666 iterations.

Table 3: Performance comparison of Qwen2.5-1.5B across five random seeds. The Goldilocks method consistently outperforms the baseline, achieving higher final performance in fewer iterations.

Method	Iterations	Scores (5 Seeds)	Mean \pm Std
GRPO Baseline	26,666	30.6, 30.5, 30.4, 29.4, 30.2	30.2 \pm 0.48
Goldilocks (Ours)	20,000	33.4, 32.9, 32.4, 32.6, 33.7	33.0 \pm 0.54

Figure 6 visualizes the learning curves averaged over the five seeds. The trajectory confirms that the Goldilocks method maintains a stable and significant lead throughout the training process.

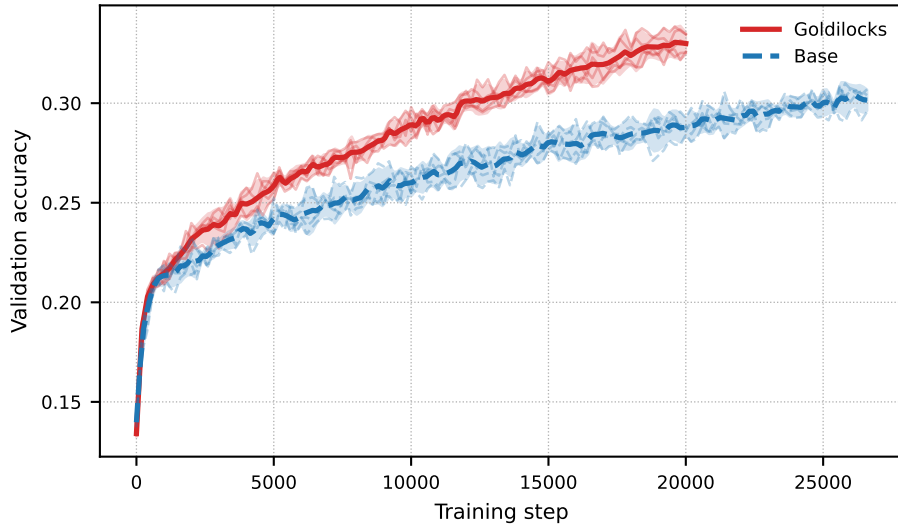


Figure 6: Learning curves for the Qwen2.5-1.5B model across five random seeds. Solid lines represent the mean performance, while the shaded regions indicate the 95% confidence intervals.

F Additional Validation Accuracy Results

This section provides extended evaluation metrics corresponding to the optimization process discussed in the main text. Specifically, we detail the validation accuracy trajectories of the baseline GRPO model Qwen2.5-1.5B compared with the Goldilocks Student Qwen2.5-1.5B and Teacher Qwen2.5-1.5B.

Figure 7 illustrates the validation accuracy as a function of total wall-clock training time (in hours), highlighting the comparative time efficiency of the respective models.

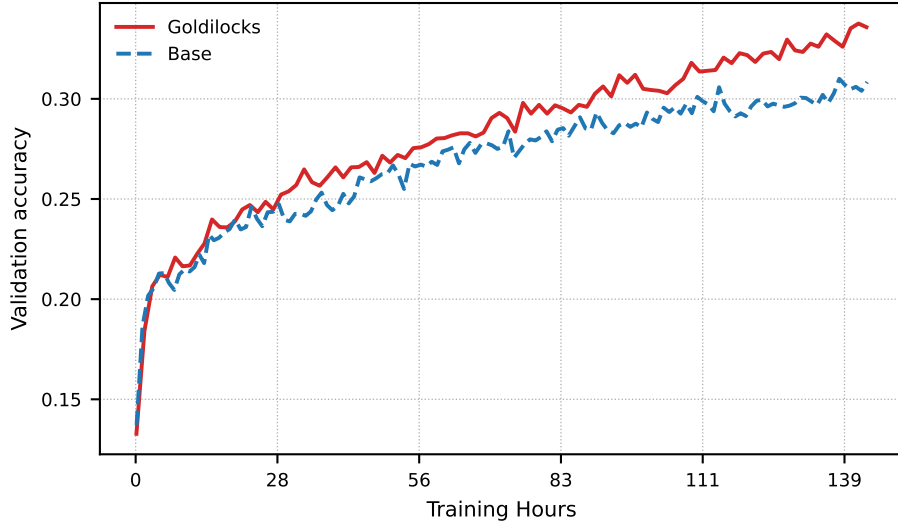


Figure 7: Validation accuracy evaluated against total training hours. The curves contrast the baseline GRPO model Qwen2.5-1.5B with the Goldilocks Student Qwen2.5-1.5B and Teacher Qwen2.5-1.5B throughout the optimization process.

Furthermore, Figure 8 depicts the validation accuracy measured against the total number of generated tokens. This perspective provides further insight into the sample efficiency of the Goldilocks variants compared to the baseline.

G Ablation Studies Plots

In this section, we provide the detailed training dynamics corresponding to the ablation experiments discussed in the main text.

G.1 Validation Accuracy

Figure 9 illustrates the evolution of validation accuracy on the held-out OpenMathReasoning validation set over the course of training. Goldilocks demonstrates a steeper learning curve compared to the GRPO baseline in all settings.

G.2 Data Efficiency (Zero-Variance Fraction)

Figure 10 plots the fraction of training questions that yield zero variance in rewards (either all correct or all incorrect). Goldilocks consistently maintains a lower rate of zero-variance in all settings.

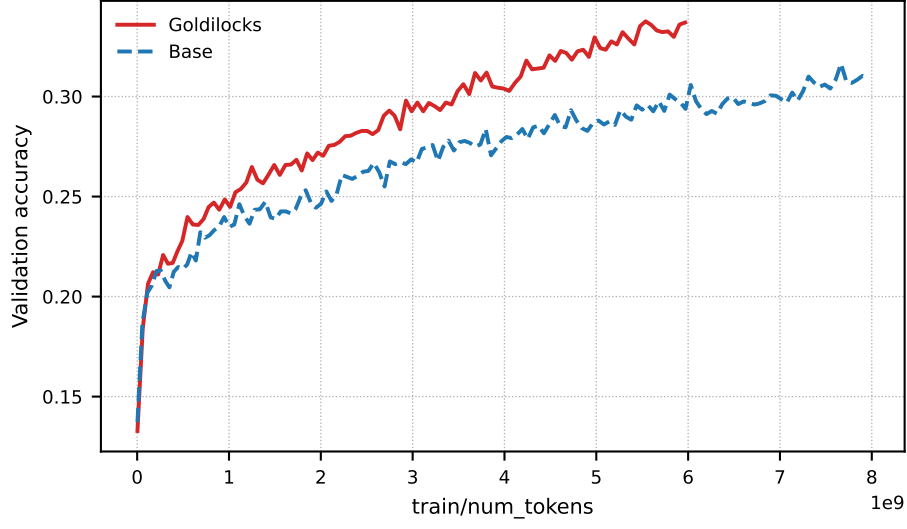


Figure 8: Validation accuracy evaluated against total generated tokens. The curves contrast the baseline GRPO model Qwen2.5-1.5B with the Goldilocks Student Qwen2.5-1.5B and Teacher Qwen2.5-1.5B throughout the optimization process.

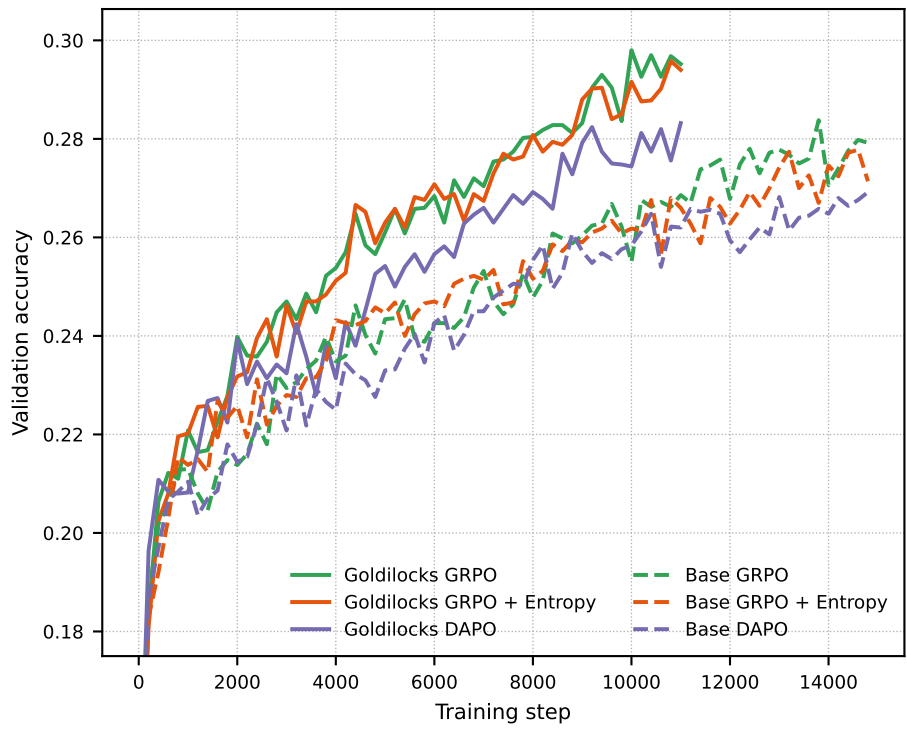


Figure 9: Validation accuracy over training steps.

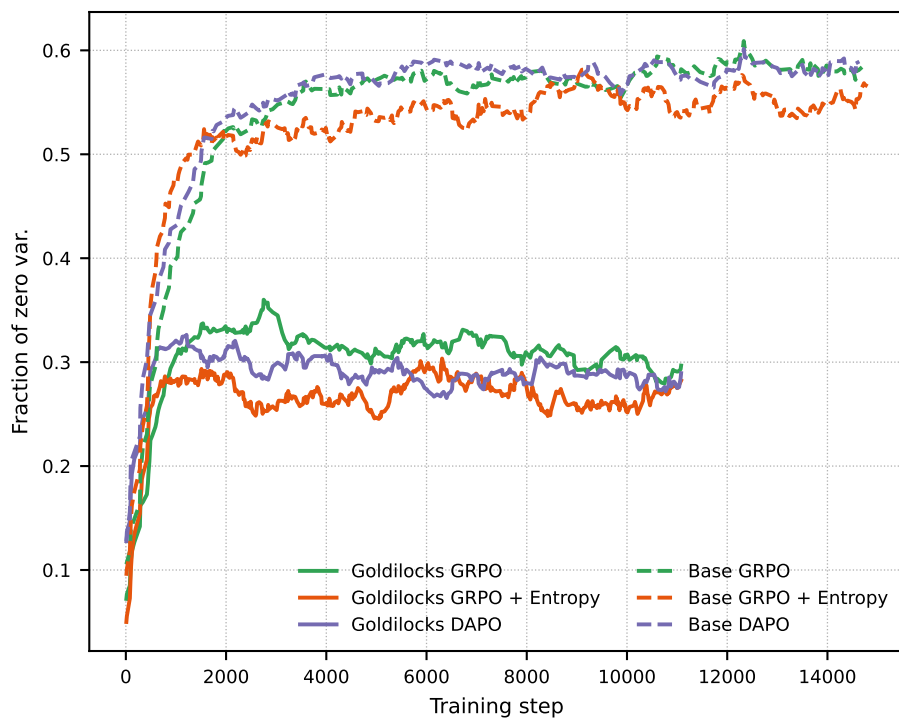


Figure 10: Fraction of questions yielding zero reward variance.

H Extended Analysis of Training Dynamics

In this section, we provide additional visualizations of the training dynamics across evaluated model families. For each architecture, we present the evaluation accuracy on the validation set, the fraction of training samples yielding zero reward variance, and the mean training rewards.

H.1 Olmo2-1B Dynamics

Figure 11 illustrates the training progression for the Olmo2-1B model. Notably, the Goldilocks teacher successfully identifies samples that maintain the training reward near the optimal 0.5 threshold, minimizing redundancy and facilitating a more efficient climb in evaluation accuracy.

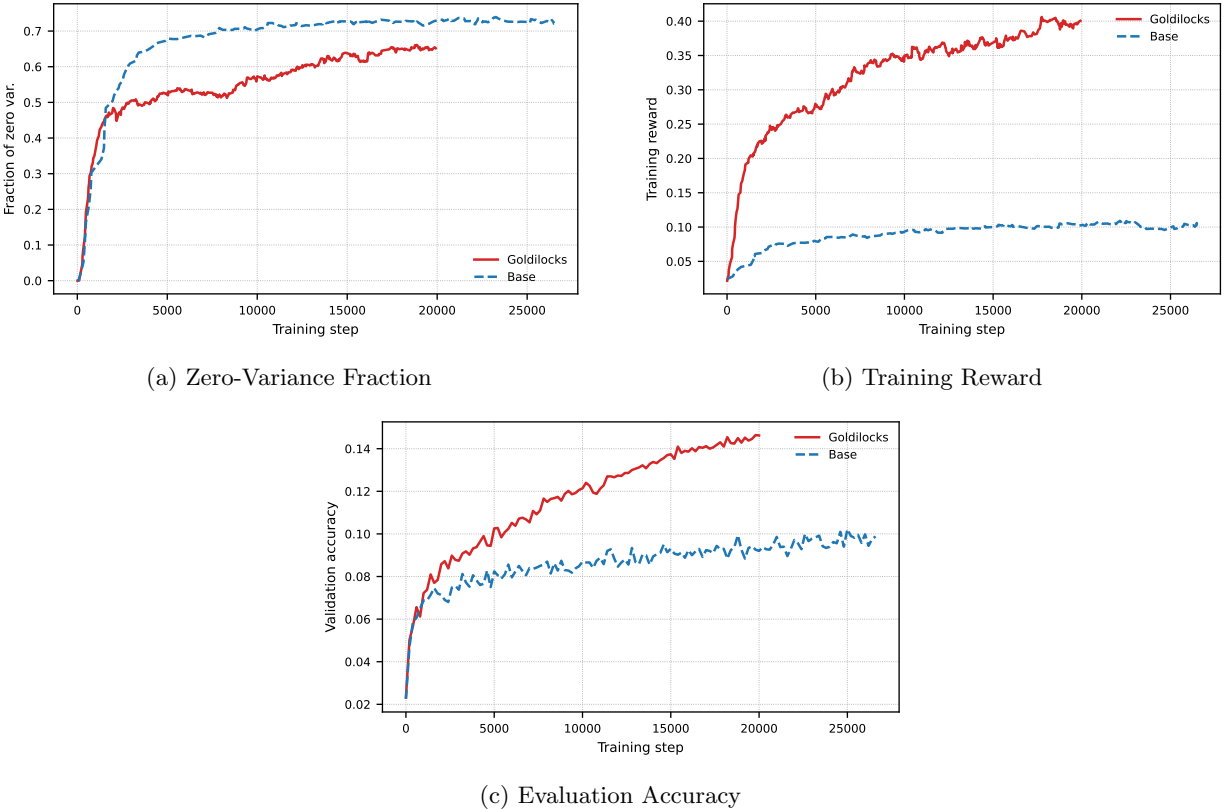
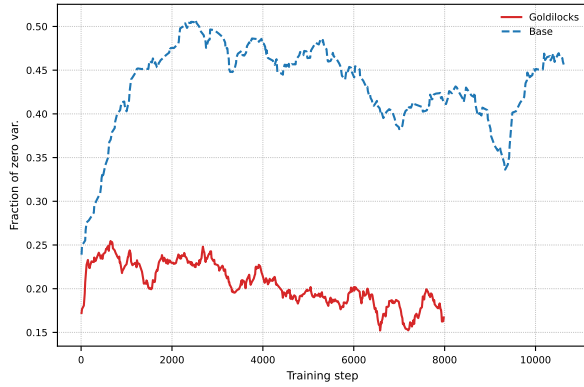


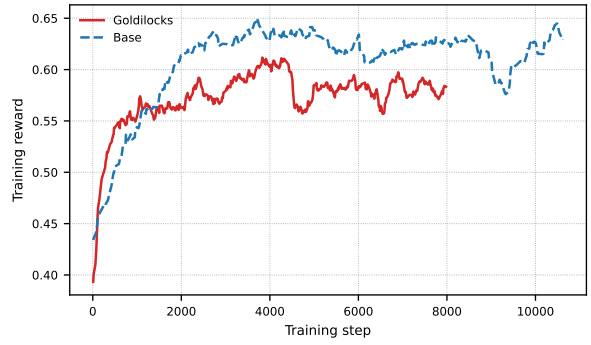
Figure 11: Training dynamics for Olmo2-1B.

H.2 Qwen3-4B Dynamics

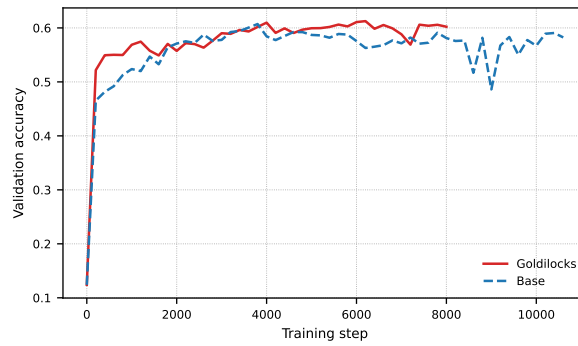
The training dynamics for the Qwen3-4B model are presented in Figure 12. Specifically, the results demonstrate that even when the average reward exceeds 0.5, Goldilocks sampling actively shifts the distribution back toward the 0.5 threshold. This behavior effectively filters out “trivial” samples, those that the model has already mastered, thereby prioritizing questions with higher informational signal and reducing computational waste on solved instances.



(a) Zero-Variance Fraction



(b) Training Reward



(c) Evaluation Accuracy

Figure 12: Training dynamics for Qwen3-4B.

H.3 Phi-4-mini-Instruct Dynamics

Figure 13 details the performance of the Phi-4-mini-Instruct model. The curriculum strategy significantly reduces the time spent on zero-variance samples, resulting in higher final validation set performance.

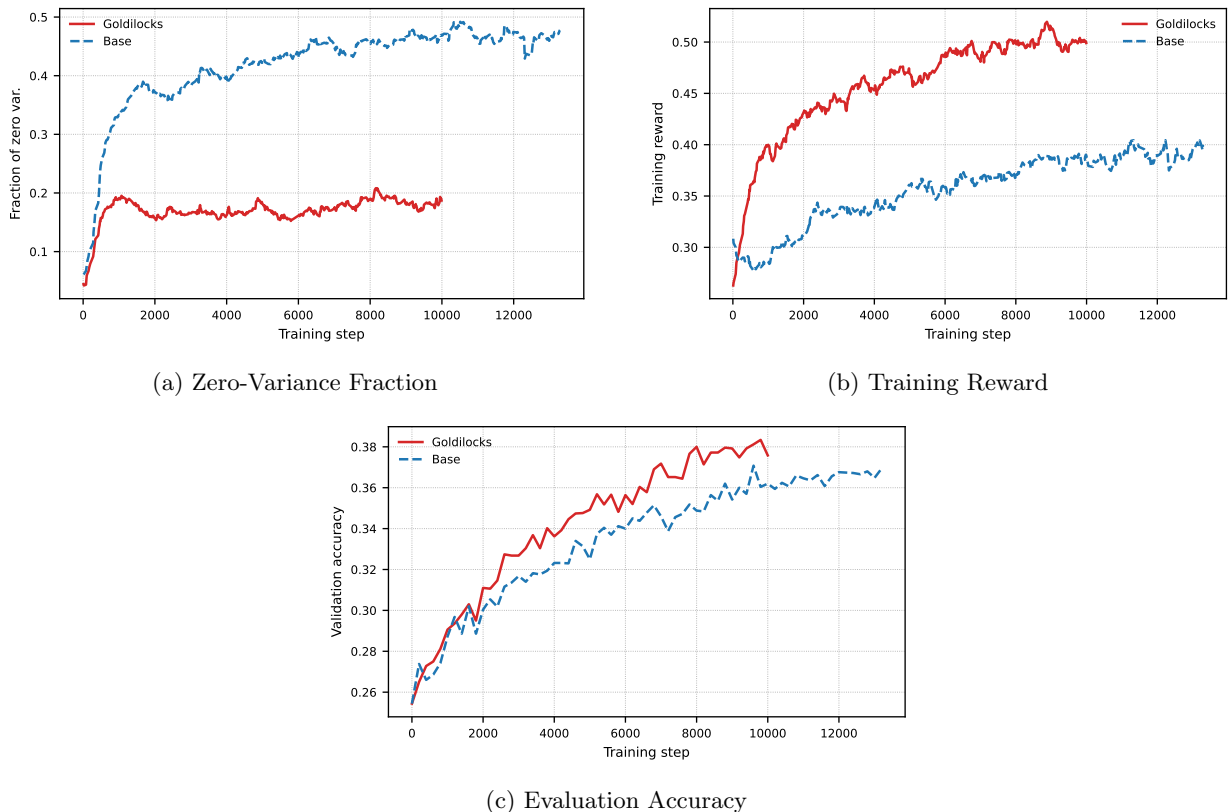


Figure 13: Training dynamics for Phi-4-mini-Instruct.

I Compute Budget and Experimental Scope

Each GRPO training run in this paper consumes approximately 1,000 GPU hours on H100/B200 hardware (Appendix K.4). Because OpenMathReasoning contains over 3 million problems, training runs are long, and the total compute footprint across all reported experiments already approaches $\sim 23,000$ GPU hours (Table 4). At this cost, adding a second benchmark of comparable scale would have required either halving the number of evaluated model families or substantially shortening each run, both of which we judged more damaging to the reliability of our conclusions than restricting the main evaluation to a single large reasoning corpus. We instead prioritized depth across four model families (1B–4B parameters) and extended runs that reach the regime where zero-variance batches dominate.

To compensate for the single-benchmark scope, we invest the available compute into three forms of evidence that are individually more informative than a shallow second-benchmark evaluation: (i) multi-seed results on Qwen2.5-1.5B (Appendix E), which back our reported gains with run-to-run variance estimates rather than single-run point measurements; (ii) training-dynamics diagnostics (zero-variance fraction, gradient norm, and reward standard deviation; Section 5.3) that directly verify the mechanistic prediction of Section 2, explaining *why* Goldilocks helps in a way that is architecture and dataset agnostic; and (iii) evaluation under two alternative loss formulations (DAPO and entropy-regularized GRPO; Section 6), which confirms that the gain stems from the curriculum itself rather than from any specific feature of vanilla GRPO. Extending Goldilocks to additional reasoning domains (code generation, theorem proving) is left to future work (Section 8).

Table 4: Approximate compute footprint of the experiments reported in this paper. Each run is a single end-to-end training trajectory at $\sim 1,000$ GPU hours.

Experiment block	Runs	GPU hours
Main results (Table 1)	8	$\sim 8,000$
Multi-seed robustness (Appendix E)	8	$\sim 8,000$
Loss/regularizer ablations (Section 6)	4	$\sim 4,000$
Teacher architecture ablations (Appendix L)	3	$\sim 3,000$
Total	23	$\sim 23,000$

J Dataset Details

For our evaluation, we constructed a fixed validation set by randomly sampling 5,000 problems from the NVIDIA OpenMathReasoning dataset (<https://huggingface.co/datasets/nvidia/OpenMathReasoning>), ensuring it is strictly disjoint from the training set. To guarantee a consistent comparison, this exact subset is used across all experiments.

K Implementation Details

K.1 Training Configuration

We maintain a consistent global batch size of 288 across all experiments. The training infrastructure varies slightly between methods to accommodate the teacher model in the Goldilocks framework. Specifically, the GRPO baseline is distributed across 8 GPUs, whereas the Goldilocks student is distributed across 6 GPUs (reserving resources for the teacher).

Gradient accumulation steps are dynamically adjusted to preserve the fixed global batch size of 288 based on the model size and available devices:

- **Small Models:** We use a per-device batch size of 4.
 - *Goldilocks (6 GPUs)*: Gradient accumulation is set to $288/(4 \times 6) = 12$ steps.
 - *GRPO (8 GPUs)*: Gradient accumulation is set to $288/(4 \times 8) = 9$ steps.
- **4B Models:** We use a per-device batch size of 3.
 - *Goldilocks (6 GPUs)*: Gradient accumulation is set to $288/(3 \times 6) = 16$ steps.
 - *GRPO (8 GPUs)*: Gradient accumulation is set to $288/(3 \times 8) = 12$ steps.

K.2 Hyperparameters

Table 5a lists the hyperparameters used for the Student model (and the GRPO baseline), while Table 5b details the specific hyperparameters for the Goldilocks Teacher.

K.3 Code details

We implemented the framework using a decoupled client-server architecture to efficiently manage the interaction between the Student and Teacher models. We found that the most robust approach is to isolate these components into two distinct processes:

- **Teacher Process (Server):** Acts as a central server that manages the curriculum and the replay buffer. It listens for requests from the student process.
- **Student Process (Client):** Runs the standard RL loop. When a new training sample is required, the student sends a request to the teacher.

Table 5: Hyperparameters for the experiments. Left: Student Policy and GRPO Baseline. Right: Goldilocks Teacher Model.

(a) Student Policy & GRPO Baseline		(b) Goldilocks Teacher Model	
Hyperparameter	Value	Hyperparameter	Value
Learning Rate	1.0×10^{-5}	Learning Rate	1.0×10^{-6}
Max Prompt Tokens	1024	Per-Device Batch Size	8
Max Completion Tokens	2048	Training Epochs per Update (E_{teacher})	4
Number of Generations (G)	16	Candidate Set Size ($K_{\text{candidate}}$)	8
Temperature (Sampling)	0.7	Epsilon (ϵ)	0.2
Temperature (Evaluation)	0.0	Replay Buffer Capacity (N_{replay})	64
KL Coefficient	0.0	Update Frequency (M_{update})	4
Update Iterations	1	Loss Function	MSE
LoRA	False		
Evaluation Frequency	200 steps		

The communication workflow operates as follows:

1. **Sample Request:** The student requests a new problem q from the teacher. The teacher selects a question based on its current utility estimates and sends it to the student.
2. **Feedback Loop:** After the student generates rollouts and computes the rewards for q , it sends these results back to the teacher.
3. **Asynchronous Updates:** The teacher aggregates this feedback into its replay buffer. Once the number of received samples reaches, the teacher triggers its own optimization step to refine the utility predictor f_ϕ .

This design allows for flexible scaling, as the heavy computation of the student (generating rollouts) is decoupled from the logic of the teacher’s selection and update mechanism.

K.4 Hardware and Computational Cost

Our experiments were conducted using NVIDIA H100 and B200 GPUs. Specifically, the larger 4B model variants were trained on B200 nodes. The average training run was approximately 1000 GPU hours for both GRPO and Goldilocks framework.

K.5 Training Steps and Accuracy Reporting

Each model variant was trained for a fixed number of steps to ensure a fair comparison across experimental conditions. The total training steps for each model are detailed below:

Table 6: Training step counts for Goldilocks and Baseline configurations. Baselines are allocated $\frac{4}{3} \times$ the steps of Goldilocks.

Model	Goldilocks Steps	Baseline Steps
Olmo2-1B	20,000	26,800
Qwen2.5-1.5B	20,000	26,800
Qwen3-4B	8,000	10,800
Phi-4-mini-Instruct (4B)	10,000	13,400

L Ablation Studies on Teacher Architectures

In addition to the teacher configuration introduced in the main text, we investigated alternative architectural choices for the utility predictor f_ϕ . Specifically, we explored different embedding extraction methods and Parameter-Efficient Fine-Tuning (PEFT) strategies.

L.1 Embedding Extraction Strategy

While our primary method utilizes mean pooling over the final layer embeddings to obtain a comprehensive question representation, we also evaluated using only the final token embedding. Given that the teacher base models are autoregressively pretrained, the final token should theoretically encapsulate the semantic summary of the sequence. However, empirical results showed that this approach was less robust than mean pooling.

L.2 Frozen Encoder

To test whether the teacher’s gain requires updating the language-model backbone at all, we trained a variant in which the pretrained encoder is frozen and only the linear projection head (\mathbf{w}, b) is updated. This configuration is attractive in principle because the base-model embeddings can be precomputed and cached, eliminating the dominant cost of teacher training. Empirically, however, the frozen-encoder teacher failed to track the student’s evolving capabilities: its predictions collapsed toward the mean of the replay buffer, and the student’s training reward and validation accuracy regressed toward the GRPO baseline. Closing this gap requires the backbone itself to adapt, which only full or sufficiently expressive parameter-efficient fine-tuning can provide.

L.3 LoRA-based Training

To reduce the computational overhead of the teacher model, we experimented with Low-Rank Adaptation (LoRA) instead of full-parameter fine-tuning. We employed a high-rank configuration with the following parameters:

- **Rank (r):** 256
- **Alpha (α):** 512
- **Dropout:** 0.01

Despite the high rank, this configuration failed to match the performance of the full-parameter teacher. We observed that the teacher’s ability to accurately predict the standard deviation of rewards was significantly diminished, likely because the fine-grained semantic features required for difficulty estimation are better captured through full-model updates

M Prompts

The final input to the model is constructed by concatenating a fixed header, the specific math problem, and a fixed footer:

$$\text{Input} = \text{PROMPT_HEADER} + \text{Question} + \text{PROMPT_FOOTER}$$

The exact text used for the header and footer is provided below.

Prompt Header

You are an expert problem solver. Your task is to solve the problem by explicitly showing your detailed Chain of Thought. You must write out your reasoning step-by-step, explaining your logic for every calculation or deduction. ****Crucially, the final answer must be enclosed in a `\boxed{\dots}` command.****

Prompt Footer

Strictly follow this output format:

Step-by-Step Reasoning

<Write your detailed thought process here. Do not skip steps.>

Final Answer

\boxed{<your final answer>}

****Important: The \boxed{...} command should only contain the final, simplified numerical or symbolic answer, with no extra text or units.****